

LARGE EDDY SIMULATIONS OF AIRCRAFT WAKE VORTICES IN A STABLY STRATIFIED ATMOSPHERE.

I. De Visscher, L. Bricteux, G. Winckelmans, S. Caliaro, T. Vilbajo

Mechanical Engineering Department, Division TERM,
Louvain School of Engineering (EPL),
Université catholique de Louvain (UCL),
2 Place du Levant, 1348, Louvain-la-Neuve, Belgium
corresponding author: ivan.devisscher@uclouvain.be

ABSTRACT

In this paper, we present Large Eddy Simulation (LES) results of aircraft wake vortices evolving in a stably stratified atmosphere. The results were obtained using a pseudo-spectral Navier-Stokes solver. Three stratification cases were investigated, from moderate ($N^* = 0.75$) to very high ($N^* = 1.4$). A 3-D visualization of the flow field is also provided, for the case $N^* = 1.0$, in order to highlight the salient features of the flow. The wake vortex system time evolution is analyzed, for all cases, using global diagnostics (trajectory and circulation of the primary wake vortices). The results are compared and discussed. The results of this work will also enable the improvement and calibration of wake vortex behavior operational models, such as the Deterministic/Probabilistic wake Vortex Model (DVM/PVM, see De Visscher et al., 2008).

INTRODUCTION

As a consequence of lift, an aircraft generates a wake that eventually forms a pair of counter-rotating vortices with circulation Γ_0 and $-\Gamma_0$, and separated by a distance b_0 , that sink under their mutual influence. It has been shown, in previous numerical studies (Holzäpfel and Gerz, 1999, Holzäpfel et al., 2001, and Nomura et al., 2006), that the thermal stratification induces a deceleration of the vortex descent rate, followed by a rising up in some cases, and that it also significantly enhances the wake circulation decay.

The aim of this investigation is to address the influence of the atmosphere stable stratification on the wake vortex behavior (position and circulation). This is of major interest to Air Traffic Management (ATM) as the strong rolling moment induced by those wake vortices on a following aircraft entering the wake can be hazardous. For that purpose, Large Eddy Simulations (LES) of wake vortices, at very high Reynolds number, are performed with various stratification levels. The results of this investigation will also be used to further improve and calibrate operational models for predicting the wake vortex behavior (transport and decay). Since the stratification has a strong impact on wake vortex transport and decay, a good real-time modeling of the phenomenon is indeed of primary importance.

GOVERNING EQUATIONS AND NUMERICAL METHOD

The governing equations are the Navier-Stokes equations for incompressible flows, using the Boussinesq approxima-

tion, and supplemented by a subgrid scale (SGS) model:

$$\nabla \cdot \mathbf{u} = 0 \quad (1)$$

$$\frac{\partial \mathbf{u}}{\partial t} + (\mathbf{u} \cdot \nabla) \mathbf{u} = -\nabla P + \nu \nabla^2 \mathbf{u} + \nabla \cdot \boldsymbol{\tau}^M + g\beta \tilde{\Theta} \mathbf{e}_z \quad (2)$$

$$\frac{\partial \tilde{\Theta}}{\partial t} + (\mathbf{u} \cdot \nabla) \tilde{\Theta} + w \frac{d\tilde{\Theta}}{dz} = \alpha \nabla^2 \tilde{\Theta} - \nabla \cdot \mathbf{q}^M \quad (3)$$

where $\mathbf{u} = (u, v, w)$ is the LES velocity field, $P = \frac{p}{\rho}$ the reduced pressure, ν the kinematic viscosity, $\boldsymbol{\tau}^M$ the SGS stress tensor model, g the acceleration due to gravity, β the thermal expansion coefficient, α the thermal diffusivity and \mathbf{q}^M the SGS heat flux model.

The potential temperature Θ has here been decomposed into the mean vertical profile and the deviation around this mean:

$$\Theta(\mathbf{x}, t) = \bar{\Theta}(z) + \tilde{\Theta}(\mathbf{x}, t), \quad (4)$$

with $\frac{d\bar{\Theta}}{dz}$ constant. This enables to perform the simulations in a periodic domain.

Pseudo-spectral Navier-Stokes solver

The Navier-Stokes solver considered here is based on the Fourier-Galerkin pseudo-spectral methodology. The spectral approximation of the velocity vector \mathbf{u} is symbolically written as

$$\mathbf{u}(\mathbf{x}, t) = \sum_{\mathbf{k}} \hat{\mathbf{u}}(\mathbf{k}, t) \exp(i \mathbf{k} \cdot \mathbf{x}), \quad (5)$$

where the spatial wavenumber vector is $\mathbf{k} = (k_x, k_y, k_z)$. The “ $\hat{\cdot}$ ” notation is used to identify Fourier transforms.

The time integration of equations (2) and (3) are carried out in spectral space using a technique in which the convective and subgrid scale model terms are marched explicitly using the 3rd order Williamson scheme. The nonlinear terms are evaluated using a pseudo-spectral algorithm and the dealiasing is done using a phase shift procedure as explained in Canuto et al., 1988. The incompressibility constraint (i.e., the effect of ∇P), Eq. (1), is satisfied by reprojecting onto a divergence free field.

High order hyperviscosity SGS model

The hyperviscosity formulation used in this study provides a SGS dissipation term acting solely at the small scales of the LES grid, without affecting the large to medium scale dynamics. The SGS model is taken as:

$$\tau_{ij}^M = (-1)^p \nabla^{2p} (2\nu_h S_{ij}) . \quad (6)$$

We here use a constant ν_h (i.e., a linear model) where

$$\nu_h = \frac{1}{T_0} C^{(p)} h^{2(p+1)}, \quad (7)$$

T_0 being a global time scale. One then obtains, in spectral space:

$$\widehat{\nabla \cdot \boldsymbol{\tau}^M}(\mathbf{k}) = (-1)^p \nu_h (|\mathbf{k}|)^{2(p+1)} \widehat{\mathbf{u}}(\mathbf{k}). \quad (8)$$

In a similar way, we have:

$$\widehat{\nabla \cdot \mathbf{q}^M}(\mathbf{k}) = (-1)^p \alpha_h (|\mathbf{k}|)^{2(p+1)} \widehat{\Theta}(\mathbf{k}). \quad (9)$$

In the present work, we used $p = 7$ and $Pr_h = \frac{\nu_h}{\alpha_h} = 1$. Previous studies (Cocle et al., 2006 and Bricteux et al., 2007) showed that this model performs well for turbulent wake vortex simulations.

NUMERICAL SET-UP

The initial wake vortex flow is composed of a pair of vortices of circulation Γ_0 and $-\Gamma_0$, and separated by a distance b_0 . A low order algebraic velocity profile was used for each vortex:

$$\Gamma(r) = \Gamma_0 \frac{r^2}{(r^2 + r_c^2)}, \quad u_\theta(r) = \frac{\Gamma(r)}{2\pi r}, \quad (10)$$

where r_c is the radius of maximum tangential velocity: it was here set to $r_c = 0.05 b_0$ (which is fairly realistic for aircraft wake vortices after roll-up with values between 0.03 and 0.05). The vortex pair sinks initially at a velocity V_0 , also leading to the definition of a characteristic time t_0 ,

$$V_0 = \frac{\Gamma_0}{2\pi b_0}, \quad t_0 = \frac{b_0}{V_0}. \quad (11)$$

In addition to this velocity field, a random isotropic perturbation is added to this velocity field with a maximum amplitude set to $10^{-3} u_{\theta, max}$. This perturbation will quicken the development of 3-D instabilities without affecting the physics of the flow.

The stable stratification level is characterized by the Brunt-Väisälä frequency, N , defined by:

$$N^2 = \frac{g}{\Theta_0} \frac{d\bar{\Theta}}{dz}, \quad (12)$$

where Θ_0 is the reference potential temperature. In a dimensionless form, this leads to $N^* = N t_0$. Three simulations have been performed using different stratification levels: $N^* = 0.75, 1.0$ and 1.4 . The Reynolds number of the flow, $Re_\Gamma = \frac{\Gamma_0}{\nu}$, is very high so that we here perform LES "in the limit of very high Reynolds number".

The periodicity lengths are set to $L_x \times L_y \times L_z = b_0 \times 6 b_0 \times 6 b_0$ using $64 \times 384 \times 384$ grid points. The extension in the y and z directions limits the influence of the periodicity and enables to obtain valid results for large times. Moreover, since the stratification effects will lead to the creation of short wave instabilities, we can limit the periodicity length in the axial direction x . The numerical resolution is $\frac{h}{b_0} = \frac{1}{64}$, which ensures that the dynamic of the vortices is properly captured ($r_c/h \geq 3$).

RESULTS

For the vortex global characterization, we compute the diagnostics on the longitudinally averaged vorticity fields:

$$\bar{\omega}(y, z, t) = \frac{1}{L_x} \int_0^{L_x} \omega(\mathbf{x}, t) dx. \quad (13)$$

The results are presented in a dimensionless form, using b_0 , Γ_0 , V_0 and t_0 for characteristic length, circulation, velocity and time, respectively. The dimensionless time is $\tau = \frac{t}{t_0}$.

Flow visualization

We provide, in Fig. 6, a visualization of the flow, using iso-surfaces of vorticity, for the case with $N^* = 1.0$. At $\tau = 0$, one observes the two vortex cores as well as the initial perturbation. At early stages ($\tau \leq 1.0$), the wake vortices descent at a constant speed and the initial separation stays constant (as it will be further quantified hereafter). Later on, for $\tau \geq 1.0$, the production of baroclinic vorticity, of opposite sign, leads to the formation of coherent transverse vortical structures ($\tau = 1.5$). This production is confined in the Rankine oval of the vortex system. These secondary structures are subjected to short waves instabilities which grow in time ($\tau = 2.0$). These instabilities keep growing, eventually leading to a complex turbulent vortex system. At $\tau = 2.5$, the primary vortices are still coherent and surrounded by a cloud of secondary turbulent vorticity. For $\tau \geq 2.5$, the strong 3-D interaction between this secondary vorticity and the primary vortices leads to a fast decay of the primary vortex circulation (as further quantified). Moreover, in this case ($N^* = 1.0$), the secondary vorticity tends to bring the primary vortices closer to each other. This induces a stronger interaction between the vortices, also influencing the descent rate and the decay. At late stages of the flow development ($\tau \geq 3.0$), the flow is so complex that one can no longer distinguish the vortex cores on the 3-D visualizations. However, on the longitudinally averaged flow, one can still observe coherent primary vortices.

Vortex trajectories

The stratification effects have a strong impact on the vortex trajectory. In order to measure the mean displacement of the vortices, we compute the position of the vortex centroid, based on the axially averaged flow.

$$\bar{\Gamma} = \int_{\Omega} \bar{\omega}_x(y, z, t) d\Omega, \quad (14)$$

$$y_c(t) = \frac{1}{\bar{\Gamma}} \int_{\Omega} y \bar{\omega}_x(y, z, t) d\Omega, \quad (15)$$

$$z_c(t) = \frac{1}{\bar{\Gamma}} \int_{\Omega} z \bar{\omega}_x(y, z, t) d\Omega, \quad (16)$$

where Ω is a disk centered on the centroid and with a radius $r = \frac{b_0}{4}$ and $\bar{\Gamma}$ is the circulation evaluated on this area. This is thus an iterative procedure.

Figs. 1 and 2 compare, for the three investigated stratification levels, the descent height, z , and the vortex lateral separation, defined as

$$b' = y_{c, right} - y_{c, left}. \quad (17)$$

Apart from the initial perturbation, the initial flow is 2-D. For the three stratification levels, for short times ($\tau \leq 0.6$), the vortices are not disturbed by the stratification effects, hence they sink at a constant velocity V_0 with a constant lateral separation b_0 . Later on, we observe a decrease of the descent rate, controlled by the stratification level; the higher N^* , the sooner and the more pronounced is this speed reduction. For $N^* \geq 1$, the vortices even rebound: at $\tau \approx 1.4$, for $N^* = 1.4$, and at $\tau \approx 2.1$, for $N^* = 1.0$. In the $N^* = 0.75$ case, the vortices tend to rebound at time $\tau \approx 3$ but other phenomena are acting. Indeed, as observed in Fig. 2, for the cases with $N^* \leq 1$, as the vortices tend to rebound, they come closer to each other ($\frac{b'}{b_0} < 1$). This closeness of the vortices balances the stratification effects. Hence, the rebound, with $N^* = 1$ become less significant while, with $N^* = 0.75$, the vortices actually increase their

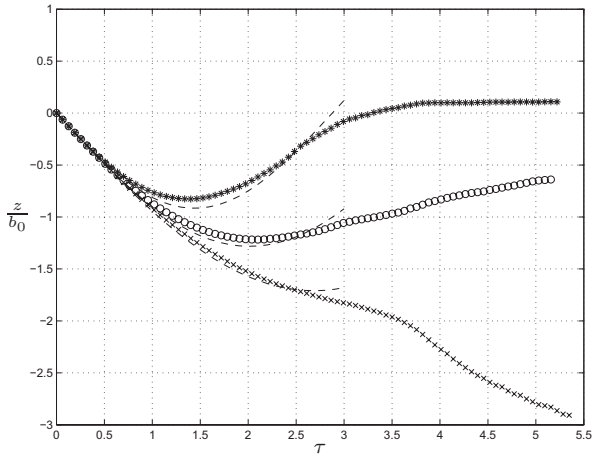


Figure 1: Time evolution of the vortex height: $N^* = 0.75$ (\times), $N^* = 1.0$ (\circ) and $N^* = 1.4$ ($*$). The results of the adapted Greene model, using $\alpha_{str} = 0.78$ in Eq. (18), is also shown (dash).

sink rate. On the contrary, for $N^* = 1.4$, the two vortices move away from each other ($\frac{b'}{b_0}$ up to 2.4), become almost independent, and rebound up to the generation altitude at $\tau \approx 3$. This is in good agreement with previous studies (see, for instance, Holzäpfel et al., 2001). It is worth to recall that, for large aircraft in low altitude, $t_0 \approx 30$ s; hence, with $N^* = 1.4$, the vortices would be back to the flight altitude after 90 s and would stay there, although decayed (see later).

The trajectory can be compared to an adaptation of the simplified trajectory model proposed by Greene (1986). In this model, the vortex altitude is described by

$$\frac{z}{b_0}(\tau) = -\frac{1}{\alpha_{str} N^*} \sin(\alpha_{str} N^* \tau). \quad (18)$$

Greene proposed $\alpha_{str} = 0.65$, based on geometrical arguments related to the Rankine oval area. However, $\alpha_{str} = 0.78$ better fits the present results for time τ up to 3, see Fig. 1, and is thus retained.

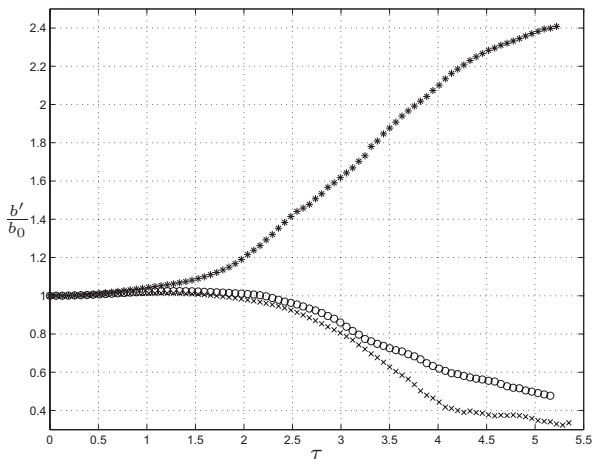


Figure 2: Time evolution of the vortex spacing: $N^* = 0.75$ (\times), $N^* = 1.0$ (\circ) and $N^* = 1.4$ ($*$).

Circulation decay

A quantity of particular importance in wake vortex related hazards is the vortex circulation: the higher the circulation, the higher the induced rolling moment on a following

aircraft. The circulation distribution $\bar{\Gamma}(r)$ is obtained by integration of the averaged axial vorticity component on a disk of radius r centered on the vortex centroid:

$$\bar{\Gamma}(r, t) = \int_0^{2\pi} \int_0^r \bar{\omega}_x(r', \theta, t) r' dr' d\theta. \quad (19)$$

Fig. 3 compare, for the three stratification levels, the circulation distribution at four times. We clearly observe a significant circulation decay, that is also function of the stratification level.

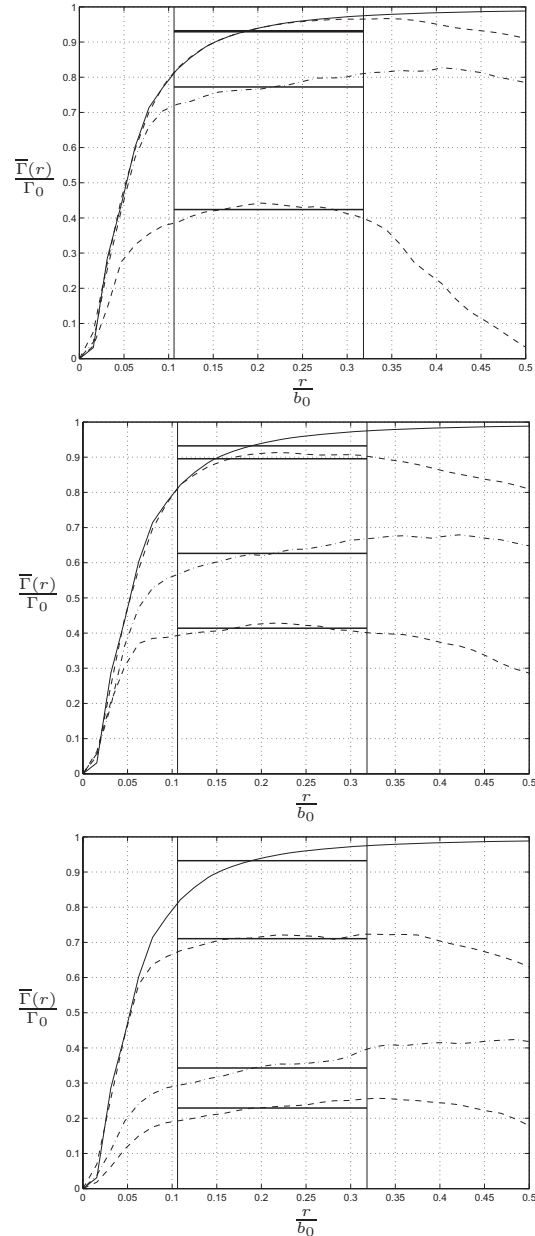


Figure 3: Circulation distribution, $\bar{\Gamma}(r)$, at time $\tau = 0$ (solid), $\tau = 2.5$ (dash), $\tau = 3.5$ (dash dot) and $\tau = 4.5$ (dash thin): $N^* = 0.75$ (top), $N^* = 1.0$ (middle) and $N^* = 1.4$ (bottom). For each time, the corresponding $\bar{\Gamma}_{5-15}$ value is also shown (thick horizontal line) in the region where it is integrated ($\frac{b}{12} \leq r \leq \frac{b}{4}$)

A usual measurement of the vortex intensity is $\bar{\Gamma}_{5-15}$, which is an average of the circulation distribution, defined as

$$\bar{\Gamma}_{5-15}(t) = \frac{6}{b} \int_{\frac{b}{12}}^{\frac{b}{4}} \bar{\Gamma}(r, t) dr, \quad (20)$$

where $b = \frac{4}{\pi} b_0$ is the wingspan of the aircraft assuming here an elliptical loading. This corresponds to what would come as post-processing of LIDAR measurements for a large aircraft (indeed taking $b = 60$ m, $\frac{b}{12} = 5$ m and $\frac{b}{4} = 15$ m). The $\bar{\Gamma}_{5-15}$ circulation values, as well as the region where they are averaged, are also provided in Fig. 3. The time evolution of the $\bar{\Gamma}_{5-15}$ is provided in Fig. 4.

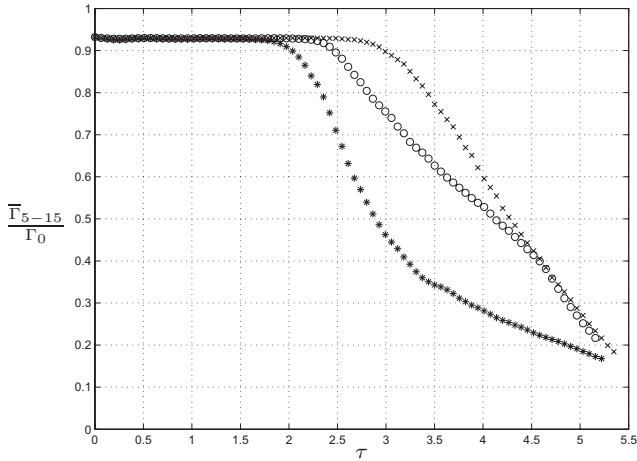


Figure 4: Time evolution of $\bar{\Gamma}_{5-15}$: $N^* = 0.75$ (\times), $N^* = 1.0$ (\circ) and $N^* = 1.4$ ($*$).

To further characterize the wake vortices, we also examine the evolution of the maximum circulation, defined as

$$\bar{\Gamma}_{max}(t) = \max_r \bar{\Gamma}(r, t). \quad (21)$$

This quantity is a good measure of the total circulation associated with the primary vortices. The time evolution of $\bar{\Gamma}_{max}$ is provided in Fig. 5.

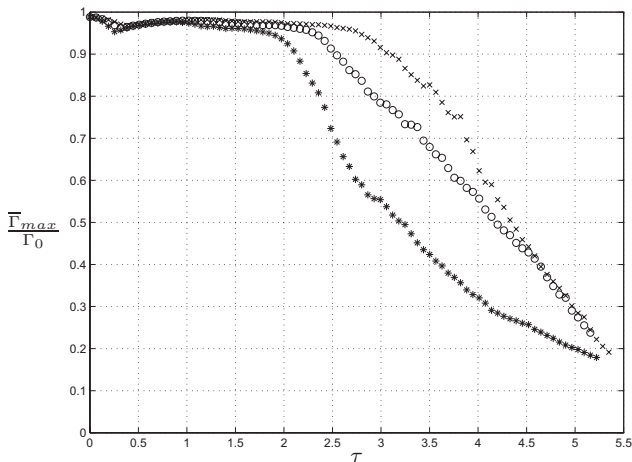


Figure 5: Time evolution of $\bar{\Gamma}_{max}$: $N^* = 0.75$ (\times), $N^* = 1.0$ (\circ) and $N^* = 1.4$ ($*$).

Using both $\bar{\Gamma}_{max}$ or $\bar{\Gamma}_{5-15}$, we clearly observe a two phase decay of the mean flow. The first decay phase is very slow, the circulation is almost conserved. This is also an indicator of the quality of the simulation: there is no spurious SGS nor numerical dissipation; the decay is solely due to the 2-D stratification effect, as seen in the $\bar{\Gamma}(r)$ evolution for short times in Fig. 3. The rapid decay phase is due to complex 3-D and turbulent interactions. The transition time between the two phases, τ_{dem} , depends on the stratification level ($\tau_{dem} \approx 2$ for $N^* = 1.4$, $\tau_{dem} \approx 2.4$ for

$N^* = 1.0$, and $\tau_{dem} \approx 2.9$ for $N^* = 0.75$). The values of those τ_{dem} are somewhat sensitive to the initial perturbation level, and should thus not be used “as such”, but the difference between the τ_{dem} for different N^* using the same initial perturbation is relevant.

The strong decay in the second phase is governed by two phenomena. First, there is the 3-D interaction between the primary vortices and the baroclinic vorticity, generated by the stratification effects, surrounding them. The decay due to this effect depends on the stratification level. This is the only decay mechanism for the case with $N^* = 1.4$. Then, it is also worth to note that, at $\tau = 3.0$, when the vortices are back to their initial altitude, the maximum circulation is $\bar{\Gamma}_{max} \approx 0.5 \Gamma_0$: the potentially encountered vortices are thus less hazardous than initially. For the cases with $N^* \leq 1$, the closeness of the primary vortices also leads to strong 3-D interaction between them and also enhances the circulation decay. The decay then also depends on the lateral distance between the vortices b' . Since b' is smaller for the case with $N^* = 0.75$ than for the case with $N^* = 1.0$, the decay rate is also higher.

CONCLUSION

We have performed numerical simulations of wake vortices interacting with a stably stratified atmosphere. We used a realistic vortex model, with relatively tight vortex cores, and a very high Reynolds number: much higher than in previous work, thus more realistic. Three stratification levels were investigated, from moderate to very high. Visualizations of the flow were used to help understand the flow dynamics and relevant diagnostics were computed to analyze and compare the wake vortex behavior in the different atmospheric conditions.

As expected, the behavior is first essentially two dimensional. Later, tridimensional interactions between the primary vortices and the instabilities generated by the stratification strongly affect the trajectory and induce turbulence, and hence fast decay.

The produced baroclinic vorticity leads the vortices to rebound and, for moderate N^* , to come closer to each other (and hence to enhance their descent rate). For moderate N^* , those effects are competing, leading to an attenuation of the vortex rebound. An adaptation of the Greene model has also been fitted on the altitude evolution. The model appears to be reliable for time up to $\tau \approx 3$.

The starting time of this rapid decay is a function of the stratification level. The decay mechanism is not identical for moderate and high stratification levels. For moderate levels, the decay is also due to the strong interaction between the two primary vortices that have been brought closer by stratification effects; for higher levels, and after vortex rebound, the vortices move away from each other, and the decay is caused by the interaction with the secondary baroclinic vorticity. In both cases, at late stages of the flow, the baroclinic secondary vorticity is mixed leading to the creation of complex turbulent structures surrounding the primary vortices and then strongly interacting with them (in fact also leading to short wave instabilities developing in the vortex cores). The stratification is thus a very efficient mechanism to destroy wake vortices. This fact is of great importance from an operational point of view. The present results also are of great importance for the improvement and calibration of the operational wake vortex models.

REFERENCES

- Bricteux, L., Cocle, R., Duponcheel, M., Georges, L., and Winckelmans, G., 2007, "Assessment of multiscale models for LES: spectral behaviour in very high Reynolds number turbulence and cases with aircraft wake vortices.", *Proc. Fifth International Symposium on Turbulence and Shear Flow Phenomena*, Vol. 1, pp. 327-331, TU München, Garching, Germany.
- Canuto, C., Hussaini, M. Y., Quarteroni, A., and Zang, T. A., 1988, "Spectral Methods in Fluid Dynamics", *Springer-Verlag*, New-York.
- Cocle, R., Dufresne, L., and Winckelmans, G., 2006, "Investigation of multiscale subgrid models for LES of instabilities and turbulence in wake vortex systems", *Complex Effects in LES: Springer volume*, LNCSE series.
- De Visscher, I., Winckelmans, G., Desenfans, O., and Lonfils, T., 2008, "Overview of UCL operational tools for predicting aircraft wake vortex transport and decay: the Deterministic/ Probabilistic wake Vortex Model (DVM/PVM) and the WAKE4D platform", *Technical Report*, Louvain School of Engineering (EPL), Université catholique de Louvain (UCL), Louvain-la-Neuve, Belgium.
- Greene, G. C., 1986, "An Approximate model of vortex decay in atmosphere", *Journal of Aircraft*, Vol. 23, pp. 566-573.
- Holzäpfel, F., and Gerz, T., 1999, "Two-dimensional wake vortex physics in the stably stratified atmosphere", *Aerospace Science and Technology*, Vol. 3, pp. 261-270.
- Holzäpfel, F., and Gerz, T., and Baumann, R., 2001, "The turbulent decay of trailing vortex pairs in stably stratified environments", *Aerospace Science and Technology*, Vol. 5, pp. 95-108.
- Nomura, K. K., Tsutsui, H., Mahoney, D. and Rottman, J. W., 2006, "Short-wavelength instability and decay of a vortex pair in a stratified fluid", *Journal of Fluid Mechanics*, Cambridge University Press, Vol. 553, pp. 283-322.

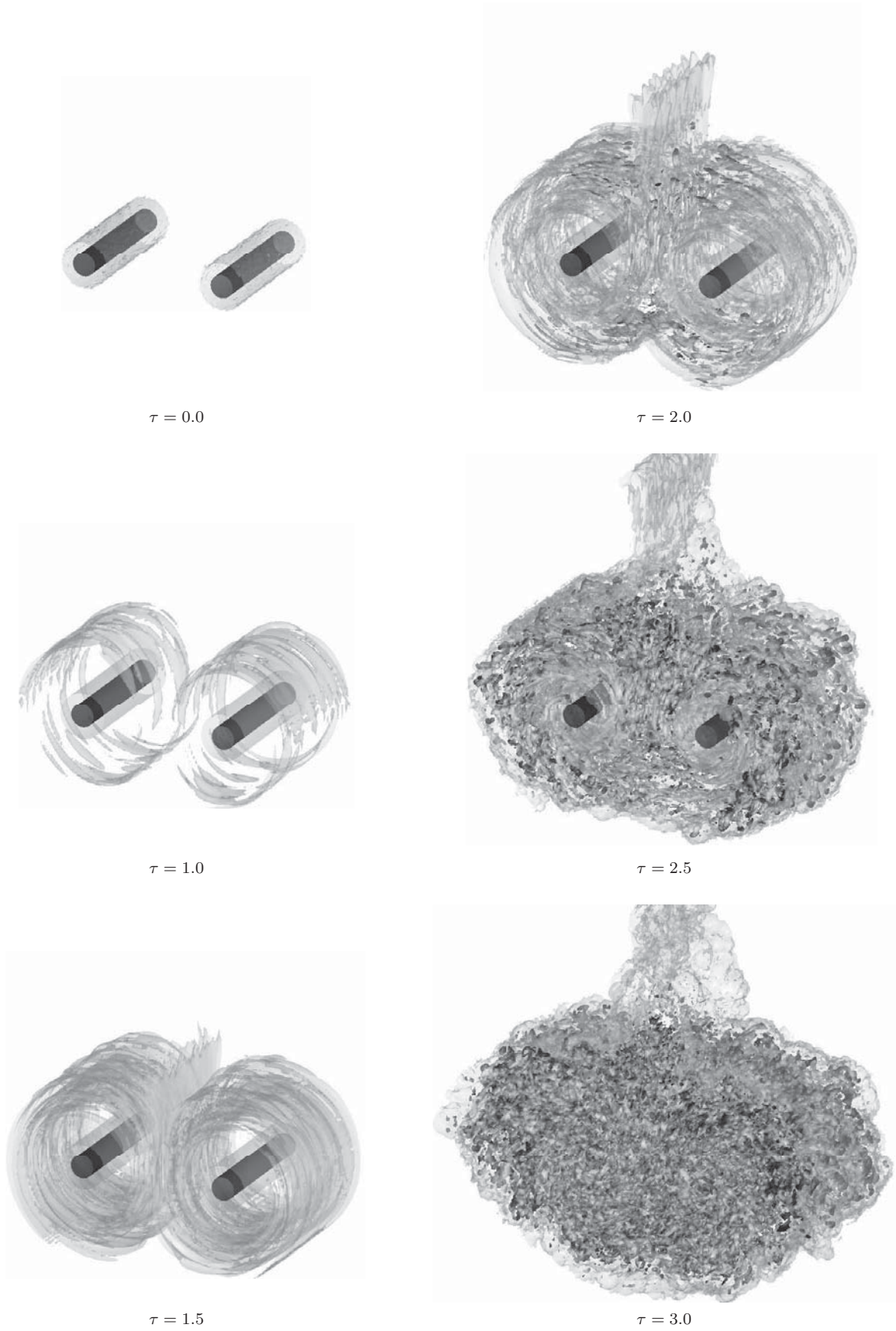


Figure 6: Case $N^* = 1.0$: iso vorticity ($\overline{\omega}_x b_0^2 / \Gamma_0$) surfaces at different times and for $\|\omega\| b_0^2 / \Gamma_0 = 1$ (low opacity) and 10 (high opacity).